Taylor & Francis
Taylor & Francis Group

The construction of a zwitterionic PVDF membrane surface to improve biofouling resistance

Xiang Shen, Yiping Zhao and Li Chen*

State Key Laboratory of Hollow Fiber Membrane Materials and Processes, School of Materials Science and Engineering, Tianjin Polytechnic University, Tianjin, China

Biofouling of membrane surfaces by the attachment of microorganisms is one of the major obstacles for ensuring the effectiveness of membrane separation processes. This work presents the construction of a zwitterionic PVDF membrane surface with improved resistance to biofouling. An amphiphilic copolymer of poly(vinylidene fluoride)-graft-poly(*N,N*-dimethylamino-2-ethylmethacrylate) (PVDF-g-PDMAEMA) was first synthesized *via* radical graft copolymerization and then the flat membrane was cast with immersed phase inversion. The PDMAEMA side chains tended to aggregate on the membrane surface, pore surface and internal pore channel surface, and were converted with 1,3-propane sultone (1,3-PS) to yield a zwitterionic membrane surface. A higher conversion of PDMAEMA chains and distribution of zwitterions were obtained using a longer treatment time. A biofouling assay indicated that incorporation of zwitterions suppressed the adsorption of extracellar polymer substances and the adhesion of *Escherichia coli* bacterial cells to the membrane surface, endowing the membrane with a high flux recovery and biofouling resistance in the filtration process.

Keywords: PVDF membrane; PDMAEMA; zwitterions; biofouling; hydrophilic

Introduction

Membrane technology is an effective toolbox for wastewater reclamation, municipal drinking water treatment and food-processing (Kovalova et al. 2012; Qin et al. 2012; Zhu et al. 2013). However, biofouling resulting from the adhesion of bacteria and subsequent formation of biofilms can lead to a marked decline in the permeation flux and increase operational costs due to frequent cleaning and maintenance (Hamzah et al. 2012; Kaneko & Funatsu 2012). The initial step in the formation of a biofilm is the non-specific and reversible attachment of bacteria to the membrane surface. Once permanently adhered, bacteria start to synthesize extracellular polymer substances (EPS) that encase the attached bacterial cells in a three-dimensional matrix. The accumulation of EPS and proliferation of bacteria facilitate the colonies developing into a mature biofilm (Herzberg et al. 2010; Bazaka et al. 2012). Thus, one of the effective approaches to eliminate biofouling is to avoid or reduce the initial adhesion of bacteria to the membrane surface (Venault et al. 2012).

Poly(vinylidene fluoride) (PVDF) is a membrane material used widely because of its excellent mechanical properties, and thermal and chemical stability. However, the intrinsic hydrophobicity of the material results in biofouling in the filtration process (Herzberg et al. 2011; Dong et al. 2012). An alternative method to resist the attachment of bacteria is the construction of a hydrophilic membrane surface tethered with hydrophilic

materials (Yang et al. 2011; Wang et al. 2012). The zwitterionic material sulfobetaine methacrylate (SBMA) has received growing attention for use in the new generation of non-fouling or low-fouling solid surfaces (Chen & Jiang 2008; Vaisocherová et al. 2008). The distinct characteristic of this material is that it contains both a positively and a negatively charged moiety within the same segment side chain. Zwitterionic structures can bind a significant amount of water molecules and thus exhibit excellent resistance to foulants. Recently, SBMA monomers were immobilized onto an existing PVDF membrane surface through atom ozone pre-activation, atom transfer radical polymerization (ATRP) and a physisorbed free radical grafting technique (Chiang et al. 2009; Chang et al. 2011; Li, Bi, et al. 2012; Li, Li, Shao, et al. 2012). Also, the copolymer of PVDF grafted with poly(sulfobetaine methacrylate) (PSBMA) had been synthesized to prepare the flat membrane *via* immersed phase inversion (Li, Li, Miao, et al. 2012). Although all the modified PVDF membranes can effectively resist the adsorption of protein, it is difficult to introduce the highly polar PSBMA into the hydrophobic membrane since they are not compatible (Ma et al. 2011). In addition, an ionically cross-linked network structure is formed due to the intra and interchain ionic contacts (Lowe & McCormick 2002), resulting in the insolubility of PSBMA in organic solvent which is suitable for PVDF. Therefore, PSBMA designed directly into the copolymer for membrane fabrication is still difficult to

---

*Corresponding author. Email: chenlis@tjpu.edu.cn

produce in practice. Lowe et al. (1996) found that SBMA could be synthesized from reaction of the monomer *N,N*-dimethylamino-2-ethyl methacrylate (DMAEMA) with 1,3-propane sultone (1,3-PS). Inspired by this process, to construct a zwitterionic membrane surface, an amphiphilic copolymer having the PDMA-EMA side chains and PVDF backbone could be synthesized for the subsequent formation of membranes. The zwitterionic structure could be constructed from the reaction of PDMAEMA with 1,3-PS to avoid the above-mentioned shortcomings. Yi et al. (2011) synthesized the PVDF-g-PDMAEMA copolymer *via* ATRP, which was used as the additive to prepare the blending membrane (PVDF/PVDF-g-PDMAEMA). The PDMAEMA side chain was further functionalized with 1,3-PS. Until now, little attention had been focused on the zwitterionization of pristine PVDF-g-PDMAEMA flat membrane. The synthesis for PVDF-g-PDMAEMA copolymer *via* radical graft copolymerization has also not been reported.

In the present work, the PVDF backbone was treated with alkali solution to produce the active functional group (C=C double bond). The PDMAEMA was grafted onto the PVDF backbones *via* radical graft copolymerization. In comparison to ATRP, this two-step process was easier to conduct as rigorous conditions were not needed. The flat copolymer membrane was first cast *via* immersed phase inversion, followed by reaction of the PDMAEMA with 1,3-PS to yield a zwitterionic membrane surface. The effects of the conversion of PDMAEMA into zwitterions on the morphology, hydrophilicity and zeta potential of the resulting membranes were investigated. The resistance of as-prepared membranes to biofouling was evaluated by monitoring EPS adsorption, bacterial adhesion and filtration performance.

Materials and methods

Materials

The PVDF powder ($M_w = 180,000$) was purchased from Solvey Co. Ltd (Brussels, Belgium). *N,N*-dimethyl formamide (DMF), poly(ethylene glycol) (PEG, 10,000) and potassium hydroxide (KOH) were kindly provided by Kermel Chemical Co. Ltd (Tianjin, China). 2,2′-azobisisobutyronitrile (AIBN) was purchased from Shisihewei Chemical Co. Ltd (Shanghai, China) and was purified from ethanol before use. DMAEMA and 1,3-PS were obtained from Aladdin (Shanghai, China). *Escherichia coli* (*E. coli*; ACCC 01625) was provided by the Institute of Microbiology (Chinese Academy of Science, China). Pure water (18 MΩ) was used for all experiments and was purified using a MilliQ system (Millipore, America). All other chemicals, unless otherwise stated, were obtained from commercial sources and used as received.

Synthesis of the PVDF-g-PDMAEMA copolymer

To synthesize the copolymer, the PVDF powder was first treated with an alkali solution (Guo et al. 2010; Feng et al. 2012). PVDF powder (50 g) was immersed in a KOH solution (350 ml, 2.5 M) with 10 ml of ethanol, and the suspension was stirred for 20 min at 60 °C. The precipitate was collected by filtration and washed (×3) with pure water. The alkali-treated PVDF powder was dried at 60 °C for future polymerization.

The copolymer was synthesized *via* radical graft copolymerization. About 10 g of the alkali-treated PVDF powder was added to 100 ml of DMF. After the powder was dissolved completely, the DMAEMA monomer (0.05 M, 7.8605 g) and initiator AIBN (0.002 M, 0.328 g) were introduced into the reaction solution in a N_2 atmosphere with continuous stirring. The reaction was carried out at 60 °C for 8 h. The resultant product was precipitated with methanol and then washed with pure water to remove the residual monomers and initiators. The synthesized copolymer was dried completely in a vacuum oven at 60 °C for 72 h.

The chemical structure of the copolymer was investigated by fourier transform infrared spectroscopy (FT-IR; Tensor37, Bruker, Germany). To prepare FT-IR samples, the copolymer powder was cast onto a potassium bromide disc with the thickness of ∼0.8 mm and dried with an infrared light. The FT-IR spectrum was obtained with a microsampling IR spectrometer. Nuclear magnetic resonance proton spectra (^{1}H-NMR) were obtained on an ARX 300 instrument (Bruker, Germany) with deuterated dimethylsulfoxide as the solvent.

Preparation of membranes

The PVDF-g-PDMAEMA copolymer membrane was formed *via* conventional immersed phase inversion. The casting solution was first prepared by mixing 16 g of copolymer and 8 g of PEG in 76 g of DMF. The solutions were stirred at 60 °C for 4 h and then left for 24 h to allow them to become completely degassed. After cooling to room temperature, the casting solution was spread with a casting knife on a glass plate and subsequently immersed into a coagulation bath (water) at 25 °C. After peeling from the glass plate, the as-prepared membrane was rinsed with water, and then kept immersed until use.

1,3-PS as the quaternization agent was incorporated into PVDF-g-PDMAEMA membrane to construct the zwitterionic structure. The flat membrane was removed from the storage water and soaked in ethanol before reaction. The reactions were performed by immersing the three membrane samples (5 cm × 5 cm) into 100 ml of an ethanol solution containing 6 g of 1,3-PS at 60 °C for 8, 24, 48 and 96 h, respectively. The resultant membranes were rinsed with pure water to remove the residue monomers, and then stored in water at room temperature.

Structural and morphological characterization of the membranes

FT-IR was used to identify functional groups on the membrane surface. The surface constitutions of as-prepared membranes were analysed by X-ray photoelectronic spectroscopy (XPS; PHI5000C ESCA system, PHI Co., USA). The membranes were cut using a razor and mounted on the standard sample studs using double-sided adhesive tape. The XPS data were obtained with an electron spectrometer using 300W AlKα radiation. The core-level spectrum was calibrated by referencing to the C1s hydrocarbon peak at 284.6 eV.

The measurement of pore size was performed using a mercury porosimeter (Autopore 9500, Micromeritics, America). Every sample membrane was dried in a vacuum oven for 24 h at 60 °C. Pore size, pore size distribution and porosity data were obtained.

The surface morphology of the membranes was analysed using a scanning probe microscope system (CSPM5500, Benyuan-nano, China). The roughness parameters, including the mean roughness (R_a), the root mean-square of the Z data (R_{ms}) and the maximum height difference from the highest peak and the lowest valley (R_z), were obtained from a 10 μm^2 scan area. All these parameters could be quantitatively obtained by atomic force microscope (AFM) analysis software (SPM Console, Benyuan-nano, China).

A contact angle instrument (DSA100, Krüss, Germany) was used to measure the water contact angle of the membranes. A 5 μl water drop was placed onto the surface of the membrane whilst the whole process was recorded by a high-speed video camera. The contact angle values were then measured using the sessile drop method.

The streaming potential of the membrane was measured *via* the assembled system described previously (Takagi et al. 2000). Before measurement, the sample was soaked for 24 h in 0.001 M KCl solution. Zeta potentials were measured using 0.001 M KCl over a range of pH (3–8).

Anti-biofouling property of the membrane

Extraction of EPS

E. coli was cultured in Luria-Bertani broth (containing 10 g l^{-1} of tryptone, 5 g l^{-1} of yeast extract and 10 g l^{-1} of NaCl) at 37 °C with shaking at 200 rpm for 24 h. The final concentration was ∼10^9 cells ml^{-1}.

Bacterial cells were removed from suspension by centrifugation at 2570 g for 15 min at 4 °C and EPS was extracted from the resultant supernatant using the method reported previously (Sheng et al. 2005; Eboigbodin & Biggs 2008). The supernatant was centrifuged at 10,000 g for 30 min at 4 °C to remove any residual bacteria, before being precipitated with ethanol at −20 °C for 18 h. Thereafter, the precipitated product was collected by filtration through a 0.2 μm hydrophilic nylon filter (Millipore, Jaffrey, NH, USA). The extract was resuspended in pure water and dialyzed using a dialysis membrane of 3500 Da (Spectra/Por, ancho-Domin-guez, CA, USA). Finally, the EPS sample was lyophilized at −50 °C under vacuum (0.01 mbar) for the preparation of the EPS solution.

EPS adsorption on the membrane

To test the adsorption of EPS to the membranes, a 2.5 cm^2 sample was immersed in a glass vial containing 10 ml of EPS solution. The vials were vibrated in a shaking bath at the constant temperature of 25 °C for 24 h to reach the adsorption equilibrium. The amount of proteins and polysaccharides adsorbed onto the membrane surface was determined by the concentration difference of the solutes. The protein was evaluated using the Bio-Rad protein assay with bovine serum albumin as the standard (Bio-Rad Lab. Inc., USA; Sim et al. 2013). The absorbance at 595 nm was determined using a UV–vis spectrophotometer (UV-1601, Shimadzu, Japan). The polysaccharides were analysed using the calorimetric method *via* absorbance at 490 nm using glucose as the standard (Dubois et al. 1956). Using these assays, the concentrations of proteins and polysaccharides in the initial EPS solution were 137.5 and 144.1 mg l^{-1}, respectively.

Bacterial adhesion to the membrane

A membrane sample with a surface area of 12.5 cm^2 was soaked in 10 ml of a bacterial suspension with 10^9 cells ml^{-1} in a sterile Erlenmeyer flask. The flask was maintained at 37 °C and shaken at 100 rpm for 3 days after which the membrane sample was rinsed with phosphate buffer solution (PBS). The bacterial cells were immobilized on the membrane surface *via* 4 vol.% glutaraldehyde in PBS at 4 °C for 4 h. Subsequently, the sample was dehydrated through a series of graded ethanol-water mixtures (20, 40, 60, 80 and 100 vol.% ethanol). Field emission scanning electron microscopy (FESEM, S-4800, Hitachi, Japan) was used to observe the morphology of the membranes after a gold layer was sputtered onto the sample for 120 s using a SC7620 sputter-coater (Quorum, England).

Filtration performance of the membrane

A custom dead end filtration system was applied to characterize the permeability of the membranes. The membrane sample was pressured with pure water at 0.2 MPa for 2 h. The pressure was then lowered to 0.1 MPa and the steady pure water flux ($J_{w,\ 0}$) was obtained following Equation 1

$$J = V/At \qquad (1)$$

4   *X. Shen* et al.

where the parameter V (l) is the volume of the pure water. A (m^2) and t (h) represent the effective area of the membrane sample and permeation time, respectively.

In order to observe the permeation flux in the presence of a bacterial suspension, the filtration cell was empted and refilled with a suspension containing 10^9 cells ml^{-1} of *E. coli*. The steady permeation flux of the suspension (J_p) was obtained when this filtration process was conducted for 24 h at 0.1 MPa. Finally, the membrane was cleaned using PBS for 1 h and then the steady pure water flux ($J_{w, 1}$) was measured again. Thus, the flux recovery (FR$_w$) could be calculated from Equation 2:

$$FR_w(\%) = (J_{w, 1}/J_{w, 0}) \times 100 \qquad (2)$$

To evaluate the fouling-resistance of a membrane, the degree of flux loss (R_t) caused by the total fouling in the filtration cycle, described above was defined by Equation 3:

$$R_t(\%) = [(J_{w, 0} - J_p)/J_{w, 0}] \times 100 \qquad (3)$$

The flux loss was caused by both reversible and irreversible foulings in the cycle (R_r and R_{ir}, respectively), which were calculated by Equations 4 and 5:

$$R_r(\%) = [(J_{w, 1} - J_p)/J_{w, 0}] \times 100 \qquad (4)$$

$$R_{ir}(\%) = [(J_{w, 0} - J_{w, 1})/J_{w, 0}] \times 100 \qquad (5)$$

Results and discussion

The chemical structure and composition of the PVDF-g-PDMAEMA copolymer

The chemical structures of the pristine PVDF, alkali-treated PVDF and PVDF-g-PDMAEMA copolymer were investigated by FT-IR; spectra are shown in Figure 1. The peak at 1640 cm^{-1} (Figure 1b) was ascribed to the stretching vibration of the C=C bonds (Guo et al. 2010). In Figure 1c, the peak intensity of the C=C bonds decreased significantly, while the peak at 1730 cm^{-1} corresponding to the carbonyl group of ester bonds in the PDMAEMA chains was observed (McGinty & Brittain 2008). These results indicated that the DMAEMA monomers were grafted to the alkali-treated PVDF main chains.

The representative ^{1}H-NMR spectra of pristine PVDF and synthesized PVDF-g-PDMAEMA copolymer are shown in Figure 2. The peaks at 3.33 and 2.49 ppm are due to the presence of moisture in the solvent (Kim et al. 2008). The two peaks at the chemical shift of 2.90 and 2.25 ppm arose from head-to-head and head-to-tail bonding arrangements in the PVDF chains, respectively (Zhai et al. 2004). In comparison to the PVDF spectrum, the peak at the chemical shift of 2.19 ppm in Figure 2b
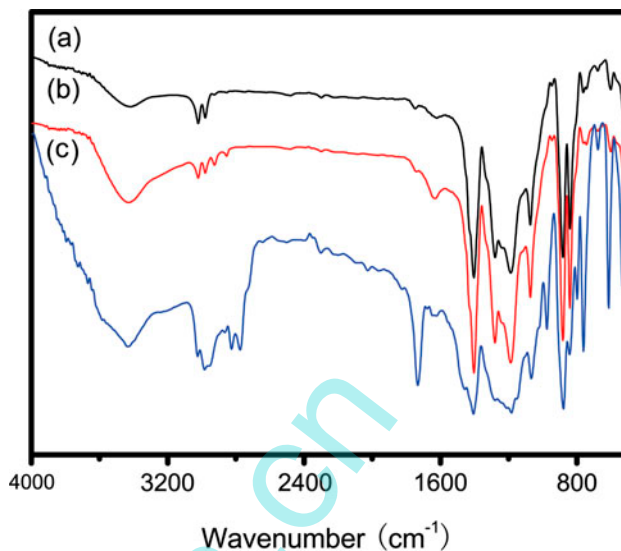

Figure 1. FT-IR spectra of (a) pristine PVDF powder, (b) alkali-treated PVDF powder and (c) PVDF-g-PDMAEMA copolymer.
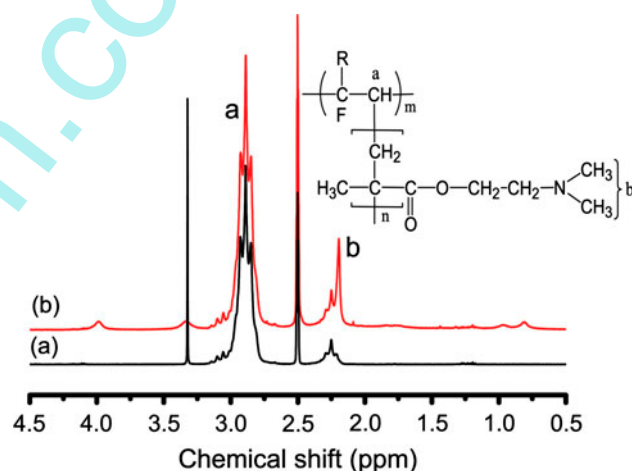

Figure 2. ^{1}H-NMR spectra of (a) PVDF and (b) PVDF-g-PDMAEMA copolymer.

corresponded to the protons of –N(CH$_3$)$_2$, which also indicated the existence of PDMAEMA chains in the copolymer (Samanta et al. 2009). The grafting degree (M_c) was defined as the number of DMAEMA units per repeat unit of PVDF and was calculated following Equation 6:

$$M_c(\%) = \{2I_b/[(6I_a - I_b) + 2I_b]\} \times 100 \qquad (6)$$

where I_a and I_b are the total intensities of the resonance for the type of each bonding environment. The M_c of PVDF-g-PDMAEMA copolymer was 8.4% based on this calculation.

The chemical compositions of the PVDF-g-PDMAEMA membrane surface

The synthesized PVDF-g-PDMAEMA copolymer was fabricated into the flat membrane *via* the immersed phase inversion method. Figure 3 shows the XPS spectra of the pristine PVDF and the PVDF-g-PDMAEMA membrane surface. It was found that, compared with the PVDF membrane, two emissions with binding energies of 399.7 and 532.3 eV were the characteristic signals of N1s and O1s on the PVDF-g-PDMAEMA membrane surface, respectively (Figure 3). The element mole percentage was determined by XPS and the percentage of carbon and nitrogen was 62.35 and 5.17%, respectively (Table 1). Thus, the concentration (the number of DMAEMA units per repeat unit of PVDF; M_s) of DMAEMA on the membrane surface could be calculated by Equation 7:

$$M_s(\%) = [2[N]/([C] - 8[N])] \times 100 \qquad (7)$$

where the factors 2 and 8 are introduced to account for the fact that there are 2 and 8 carbon atoms per repeat unit of PVDF and DMAEMA, respectively. [N] and [C] stand for the mole percentage of N and C, respectively. The value of 49.3% for M_s was substantially higher than
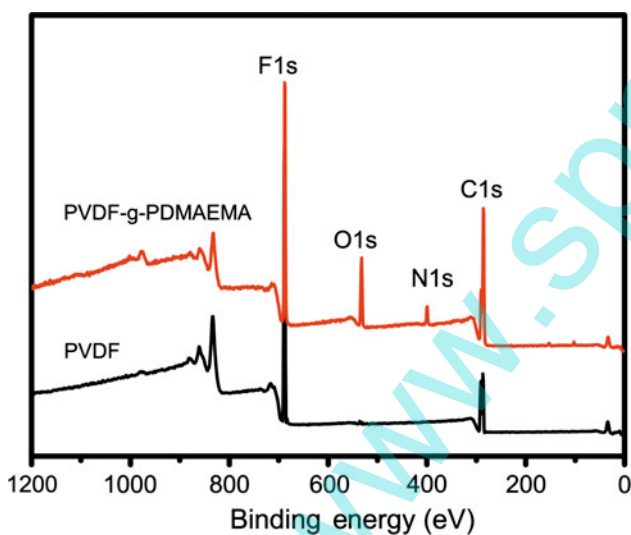

Figure 3. XPS wide-scan spectra of pristine PVDF and PVDF-g-PDMAEMA membrane surfaces.

Table 1. Surface chemical composition of PVDF-g-PDMAEMA membranes after treatment with 1,3-PS.

Treatment time (h)	C (%)	F (%)	O (%)	N (%)	S (%)	S/N (%)
0	62.35	22.45	10.03	5.17	–	–
8	60.66	22.68	11.45	4.14	1.07	25.8
24	57.45	25.13	12.14	3.51	1.77	50.4
48	57.09	27.45	10.8	2.91	1.75	60.1
96	58.11	26.14	11.04	2.69	2.02	75.1

the value of M_c of the copolymer calculated from the ^{1}H-NMR data (8.4%), indicating that the hydrophilic PDMAEMA chains were segregated onto the membrane surface, pore surface and internal pore channel surface. This was ascribed to enthalpic and entropic effects (Sui et al. 2012). The interfacial energy between water and the hydrophilic component was much lower than that between water and the hydrophobic component. During the process of membrane formation, the hydrophilic PDMAEMA chains migrated to the polymer/water interface due to the high chemical potential between the PDMAEMA and molecules of water. In addition, the hydrogen bonding interactions between the ester groups of PDMAEMA and water molecules resulted in an enthalpic preference for exposing the hydrophilic chains to the membrane and internal pore surfaces. Similar experimental results were obtained from previous studies when different amphiphilic copolymers were incorporated to prepare the membranes (Deng et al. 2010; Koh et al. 2010; Sui et al. 2012; Tao et al. 2012). This segregation behaviour was utilized to improve the surface properties of the membranes. In the present work, the aggregated PDMAEMA side chains provided the active sites for the further functionalization of the membrane surface, pore surface and internal pore channel surface.

Construction of the zwitterionic membrane surface

The zwitterionic membrane surface was designed through the reaction of PDMAEMA chains with 1,3-PS as the quaternization agent. The variation in the chemical structure of PVDF-g-PDMAEMA membrane before and after treatment was investigated and a typical FT-IR spectrum is displayed in Figure 4. The presence of sulfo groups was ascertained from the bonds of stretching
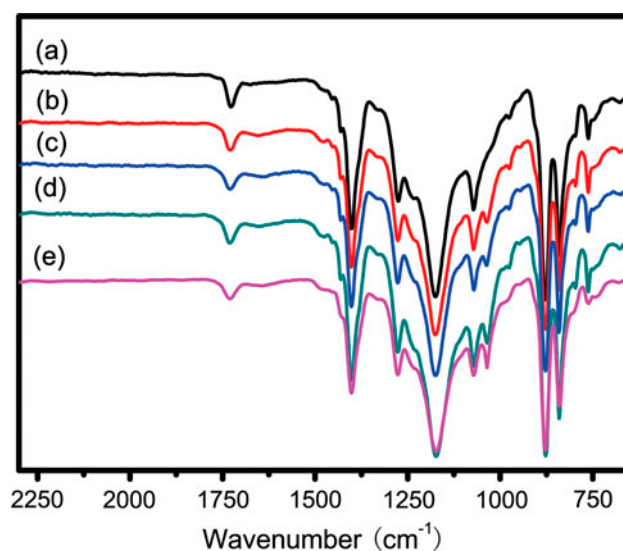

Figure 4. FT-IR spectra of PVDF-g-PDMAEMA membranes after treatment with 1,3-PS for (a) 0 h, (b) 8 h, (c) 24 h, (d) 48 h and (e) 96 h.

6   *X. Shen* et al.

vibrations at $1037\,cm^{-1}$. Clearly, the peak intensity increased with increasing treatment time from 0 to 96 h. These results implied that the 1,3-PS had been covalently immobilized.

Since the pristine PVDF-g-PDMAEMA membrane could be soaked in ethanol, which is a good solvent for 1,3-PS, the ethanol solution containing the 1,3-PS was able to permeate through the membrane pores and along the internal pore channel surfaces. Consequently, the aggregated PDMAEMA chains were converted into the zwitterionic structure. The XPS wide-scan spectra of the membranes are shown in Figure 5. The presence of the S signal at 167 eV also confirmed the successful attachment of 1,3-PS on the PVDF-g-PDMAEMA membrane surface. Figure 6 shows the typical N1s core-level spectra of as-prepared membranes. For the

pristine PVDF-g-PDMAEMA membrane, there was a single peak at 399.7 eV, originating from the tertiary amine. However, the N1s spectra of the membranes treated with 1,3-PS were cut-fitted with two peak components by multi-Gaussian functions. Except for a peak component corresponding to the N of the tertiary amine, an additional peak component at 402.5 eV was attributed to the N^+ of the quaternary amine. The appearance of these two peak components indicated that the PDMAEMA side chains were partially converted into zwitterions. The conversion of PDMAEMA side chains could be obtained from the percentage of N^+ in the total nitrogen concentration and was calculated using Equation 8:

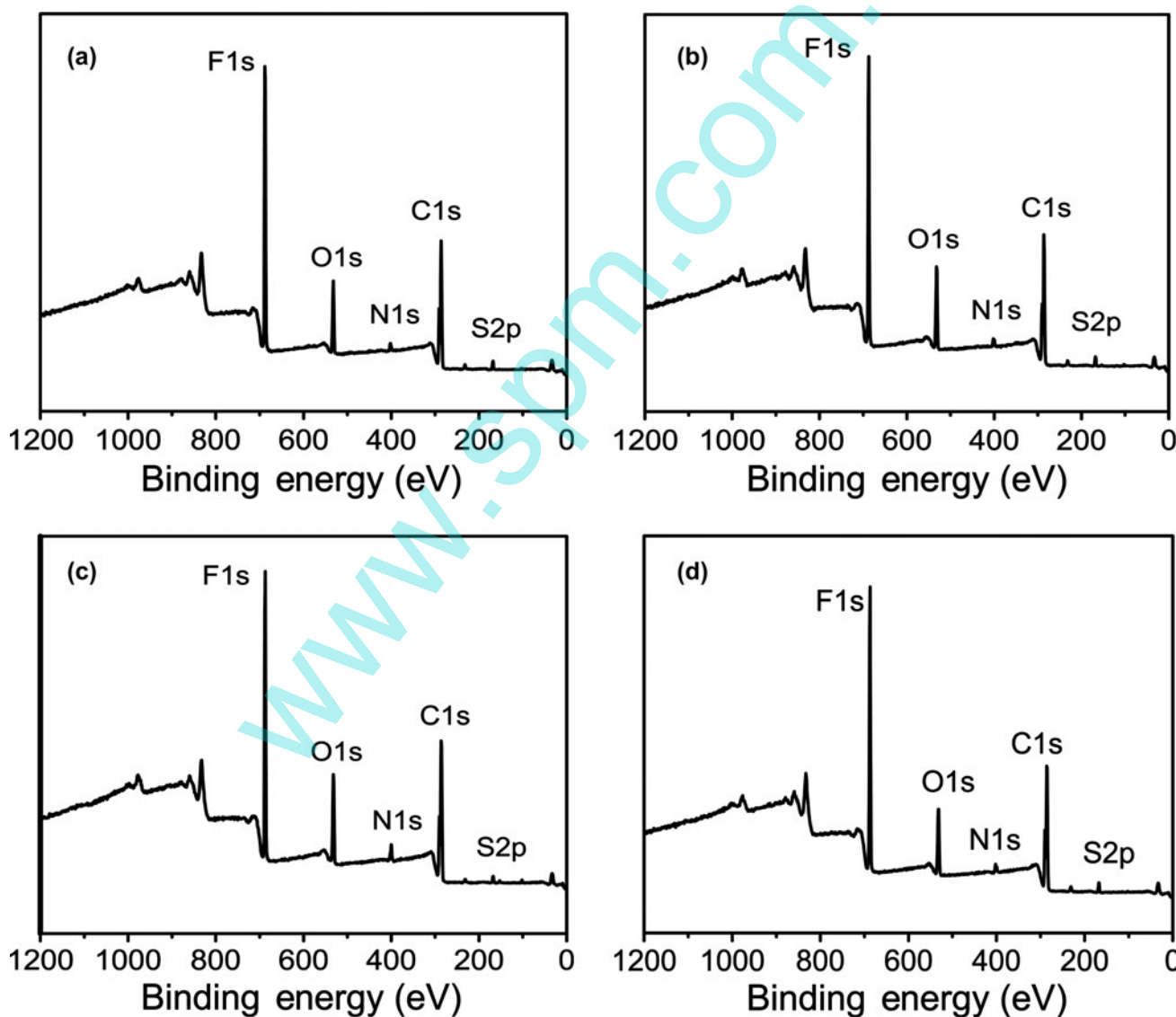$$\text{Conversion}\,(\%) = [[N^+]/([N^+] + [N])] \times 100 \qquad (8)$$

Figure 5.   XPS wide-scan spectra of PVDF-g-PDMAEMA membranes after treatment with 1,3-PS for (a) 8 h, (b) 24 h, (c) 48 h and (d) 96 h.

where [N$^+$] and [N] represent the areas of the peak components generated from the N1s core-level spectrum of the membrane surfaces. These conversions as a function of treatment time are shown in Figure 7. It was found that the conversions of the PDMAEMA chains were 23.8, 48.4, 60.9 and 75.1% when the treatment times were 8, 24, 48 and 96 h, respectively. This result was also in agreement with the S/N ratio shown in Table 1.

As the side chains had equal positively and negatively charged groups, the distribution of zwitterions could be evaluated by the unit numbers of sulfo groups at a specific area. Therefore, the distribution of zwitterions was calculated *via* Equation 9:

$$
\text{Distribution} = \{[(m_1 - m_0)/M_{1,3-\text{PS}}] \times 6.02 \\ \times 10^{23}\}/A \tag{9}
$$

where m_0 (g) and m_1 (g) are the mass of the PVDF-g-PDMAEMA membrane before and after treatment with 1,3-PS. $M_{1,3-\text{PS}}$ is the mole weight of 1,3-PS monomer. A is the specific area of the pristine PVDF-g-PDMAEMA membrane. The result is also shown in Figure 7. The zwitterions were 0, 1.5, 2.2, 3.1 and 6.0 units in every nm^2 g^{-1} when the treatment times were 0, 8, 24, 48 and 96 h, respectively. A high proportion of

zwitterions contributed to the improved biofouling resistance of the membrane (Li, Li, Miao, et al. 2012).

Membrane morphology

The structure of a membrane, including the pore structure, the pore size and distribution, can greatly affect the membrane performance (Rahimpour & Madaeni 2010). In this study, the pore size, pore size distribution and porosity of PVDF-g-PDMAEMA membranes before and after treatment were investigated *via* mercury porosimetry. The pristine PVDF-g-PDMAEMA membrane exhibited a porosity of 79.5% and a mean pore size of 163 nm (Figure 8). For the membranes treated with 1,3-PS, both the mean pore size and porosity decreased (to 131 nm and 70.1%, respectively) after treatment for 96 h. The decrease in the mean pore size and porosity provided evidence that 1,3-PS was covalently immobilized not only onto the surface of the membrane but also onto the inner pore channel surface. As ethanol was a good solvent for the monomer 1,3-PS and diffused along the membrane pore channel, the 1,3-PS monomers were covalently attached onto the membrane pore channel surface resulting in the decrease in porosity and mean pore size.

The surface morphology of the PVDF-g-PDMAEMA membrane after the treatment with 1,3-PS was evaluated by AFM. The 3D images are shown in Figure 9. The
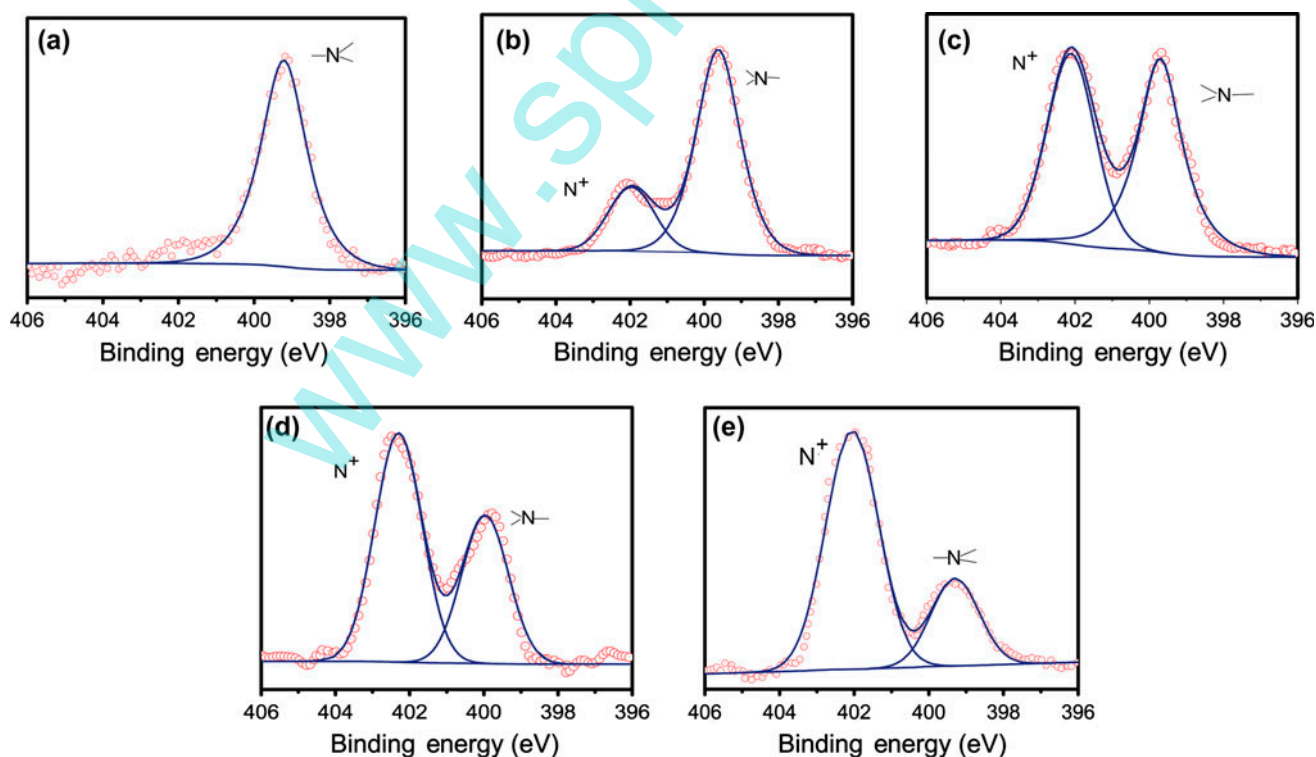

Figure 6.   N1s spectra of PVDF-g-PDMAEMA membranes after treatment with 1,3-PS for (a) 0 h, (b) 8 h, (c) 24 h, (d) 48 h and (e) 96 h.
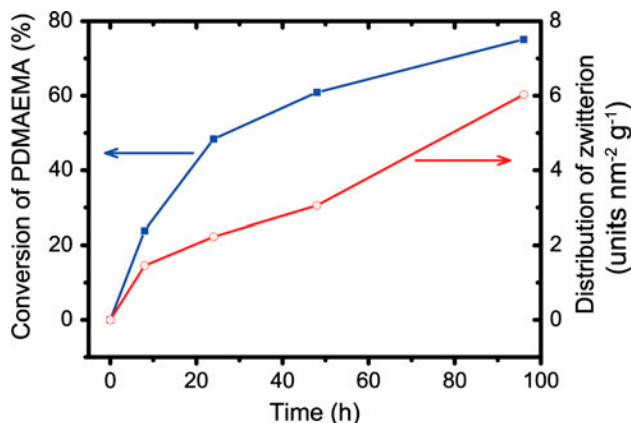
Figure 7. Conversion of PDMAEMA side chains and distribution of zwitterions.

surface roughness parameters, including R_a, R_{ms} and R_z, are summarized in Table 2. The R_a, R_{ms} and R_z values decreased with an increase in the treatment time from 0 to 96 h. The extent of the decrease for R_z was substantially higher than for R_a and R_{ms}. Similar experimental results were obtained previously (Yi et al. 2011). R_a and R_{ms} were correlated to surface pore size and surface porosity (Khulbe et al. 2004), when a membrane surface was porous, the values of R_a and R_{ms} were high. Conversely, R_z was mainly dependent on the depressions characterizing the depth of the surface pore and high

peaks characterizing the nodules. A higher R_z value can be obtained when a membrane surface consists of deeper depressions and higher peaks (Khayet et al. 2009). In the present work, pores near the membrane surface were covered or clogged due to the attachment of 1,3-PS, resulting in the decrease in the surface pore size and vertical depth of the valleys. As a result, a smoother membrane surface was exhibited and the R_z value decreased substantially with the increase in treatment time from 0 to 96 h.

Hydrophilicity and zeta potential of the membrane

The water contact angle was measured to assess the hydrophilicity of the membrane. Figure 10 shows that the contact angle for the pristine PVDF-g-PDMAEMA membrane was the highest, while the membranes treated with 1,3-PS showed lower contact angle values, indicating an increase in hydrophilicity when the PDMAEMA side chains were transformed into zwitterions. Furthermore, all the membranes exhibited a similar decreasing rate of water contact angle, which might be ascribed to the variation in membrane surface morphology and chemical structure. The water contact angle has been shown to be affected by the hydrophilicity of the membrane surface, the membrane structure including the surface pore size and wettability of internal pore channel surface (Li, Li, Miao, et al. 2012). In the present study, XPS shows that a higher number of zwitterions were distributed on the membrane and pore surfaces after
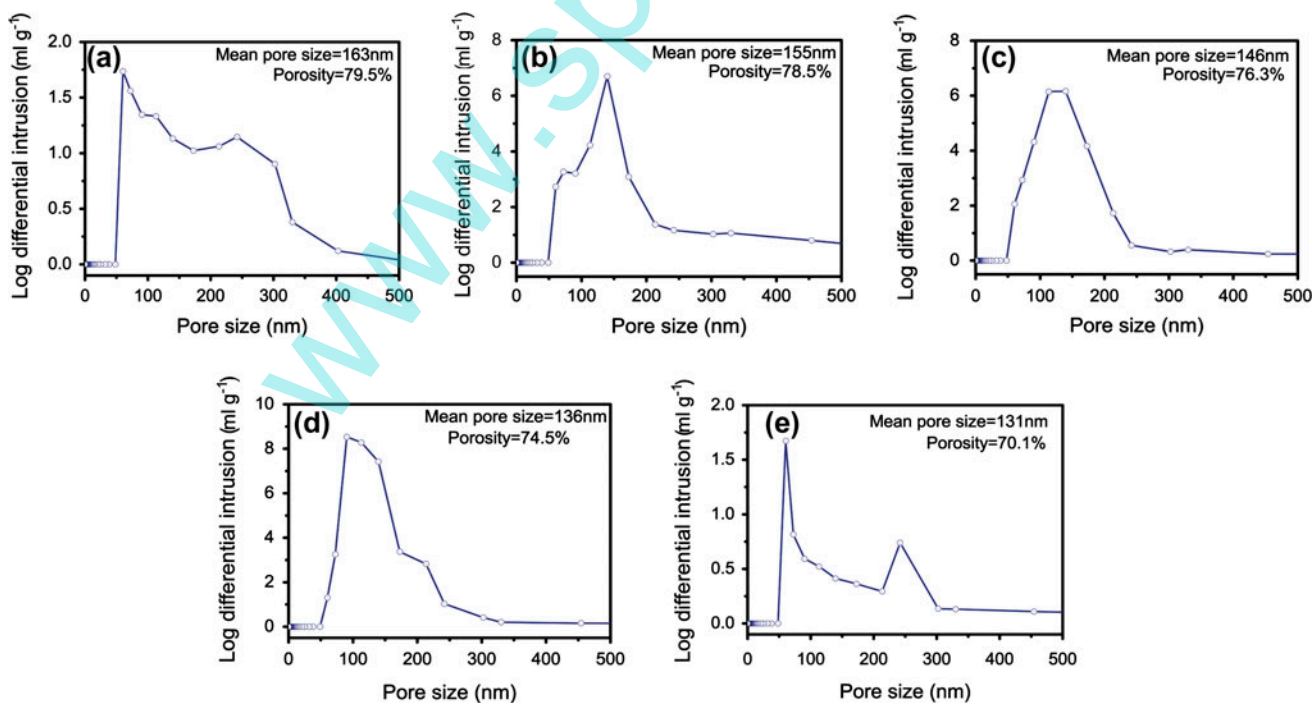

Figure 8.   Pore size and pore size distribution of PVDF-g-PDMAEMA membranes after treatment with 1,3-PS for (a) 0 h, (b) 12 h, (c) 24 h, (d) 48 h and (e) 96 h.'
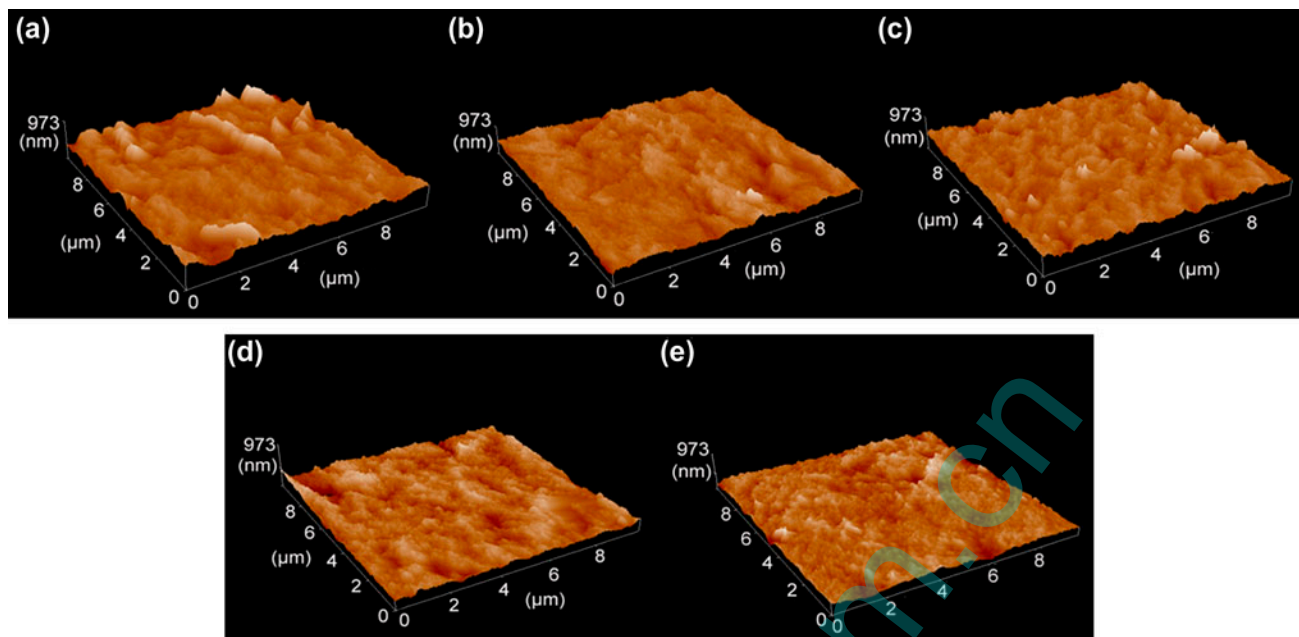
Figure 9. 3D AFM images of PVDF-g-PDMAEMA membranes after treatment with 1,3-PS for (a) 0 h, (b) 8 h, (c) 24 h, (d) 48 h and (e) 96 h.

Table 2. Roughness parameters of PVDF-g-PDMAEMA membranes after treatment with 1,3-PS.

Treatment time (h)	R_a (nm)	R_{ms} (nm)	R_z (nm)
0	50.3	69.8	661.0
8	44.0	56.8	646.0
24	42.5	56.2	550.0
48	39.9	51.9	480.2
96	36.2	45.6	469.6

Notes: R_a = mean roughness, R_{ms} = root mean-square of the Z data and R_z = maximum height difference between the lowest valley and the highest peak.

Figure 10. Water contact angle of PVDF-g-PDMAEMA membranes after treatment with 1,3-PS for (a) 0 h, (b) 8 h, (c) 24 h, (d) 48 h and (e) 96 h.

longer treatment times. When the water droplet contacted the membrane surface, the electronic interaction between the zwitterions and the water molecules resulted in an instant spread and penetration of the water drop and a reduced water contact angle. Conversely, the decrease in the size of the surface pores made the penetration of the water droplet into the membrane matrix difficult. It can be concluded that surface hydrophilicity was the leading factor affecting the decreasing rate of water contact angle.

The zeta potentials of the PVDF-g-PDMAEMA membranes are reported in Figure 11. It was found that the pristine PVDF-g-PDMAEMA membrane exhibited the biggest zeta potential, while the zeta potential of the membrane treated with 1,3-PS decreased with the increased conversion of PDMAEMA into zwitterions. As the zwitterions had balanced oppositely charged groups,
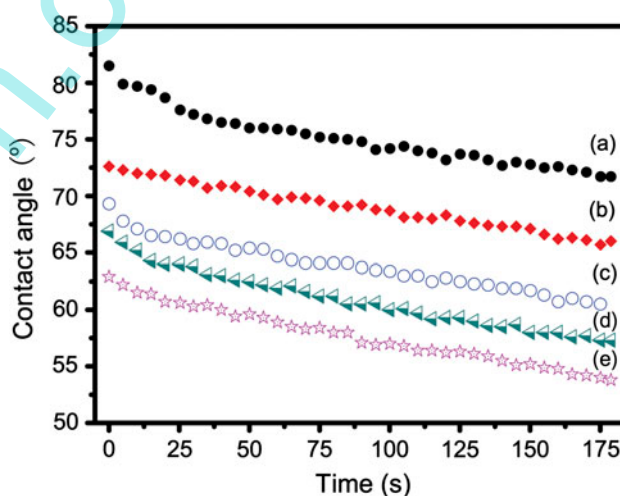
the zeta potentials of the treated membranes were ascribed to the protonation and deprotonation of residual, unconverted PDMAEMA side chains (Schepelina & Zharov 2008; Berndt et al. 2010; Yi et al. 2011). At a high pH, most of the amine groups were protonated. When the pH value increased, the deprotonation of the residual amine groups decreased the zeta potential of the membranes. Therefore, marked changes in the zeta potential were observed at between pH 3 and 5. This behaviour has been described previously (Yi et al. 2011).
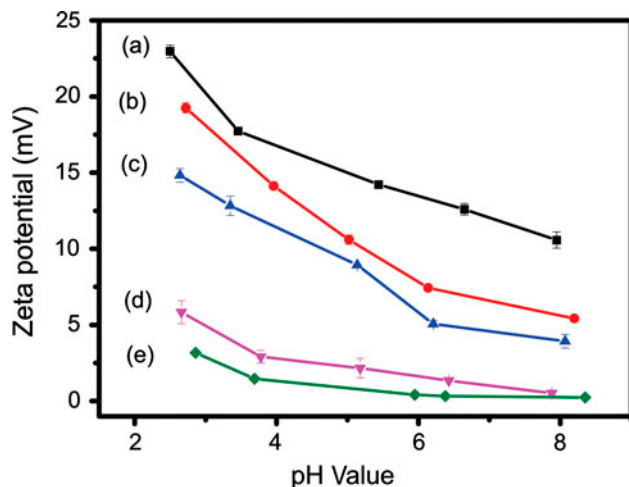
Figure 11.   Zeta potential of PVDF-g-PDMAEMA membranes after treatment with 1,3-PS for (a) 0 h, (b) 8 h, (c) 24 h, (d) 48 h and (e) 96 h.

The zeta potential values for membranes treated for 48 and 96 h were ∼0 mV. Membrane surfaces of neutral charge have generally been found to show excellent biofouling resistance (Razi et al. 2012).

Biofouling assay of the membrane

EPS are primarily composed of proteins and polysaccharides. Many studies have confirmed that the EPS is the essential element for the formation of biofilms (Cheng et al. 2009; Herzberg et al. 2010, 2011). EPS could form a gel-like matrix on the surface of a membrane, providing a biofilm with mechanical stability through hydrophobic interactions, hydrogen bonds, electrostatic forces and van der Waals interactions. In addition, the partially digestion of EPS provided sufficient energy for the proliferation of the biofilm. Biofouling can be caused by the attachment of bacteria and the formation of a biofilm. Thus, the ability to resist the adsorption of EPS is recognized as a prerequisite for a membrane surface to prevent the adhesion of bacteria (Cheng et al. 2009). In this work, the EPS was extracted from *E. coli* cells as stated earlier. The EPS adsorption of as-prepared membranes was evaluated by immersing the membrane into the EPS solution, and the amount adsorbed was determined by measuring the concentration of EPS in solution before and after the adsorption step. Figure 12 shows the adsorption of EPS by PVDF-g-PDMAEMA membranes before and after treatment. For the pristine PVDF-g-PDMAEMA membrane, the adsorption of proteins and polysaccharides was 59.8 ± 3.5 and $87.4 \pm 1.5\,\mu g\,cm^{-2}$ respectively, which was attributable to electronic interactions between the PDMAEMA side chains and the EPS macromolecules. However, the amounts adsorbed decreased when the PDMAEMA side chains were converted into zwitterions. For the membrane treated for 96 h, the amounts adsorbed decreased to $7.8 \pm 3.1\,\mu g\,cm^{-2}$ for proteins and $29.4 \pm 1.8\,\mu g\,cm^{-2}$ for polysaccharides, implying an enhanced fouling resistance. Zwitterionic surfaces are believed to be hydrated by electrostatic interaction and hydrogen bonding with water. The hydration layers on the surface of a membrane result in a strong repulsion of the EPS macromolecules that contact the surface without conformation change in a reversible manner (Ma et al. 2011). As a result, the zwitterionic membrane surfaces were responsible for the limited adsorption of EPS.

To obtain detailed information on the adhesion of bacteria to the membrane surface, the membrane samples were immersed in the bacterial suspension for 3 days to evaluate their resistance to biofouling. Figure 13 shows the typical FESEM images after adhesion of bacterial cells. It can be seen that cells of *E. coli* were deposited
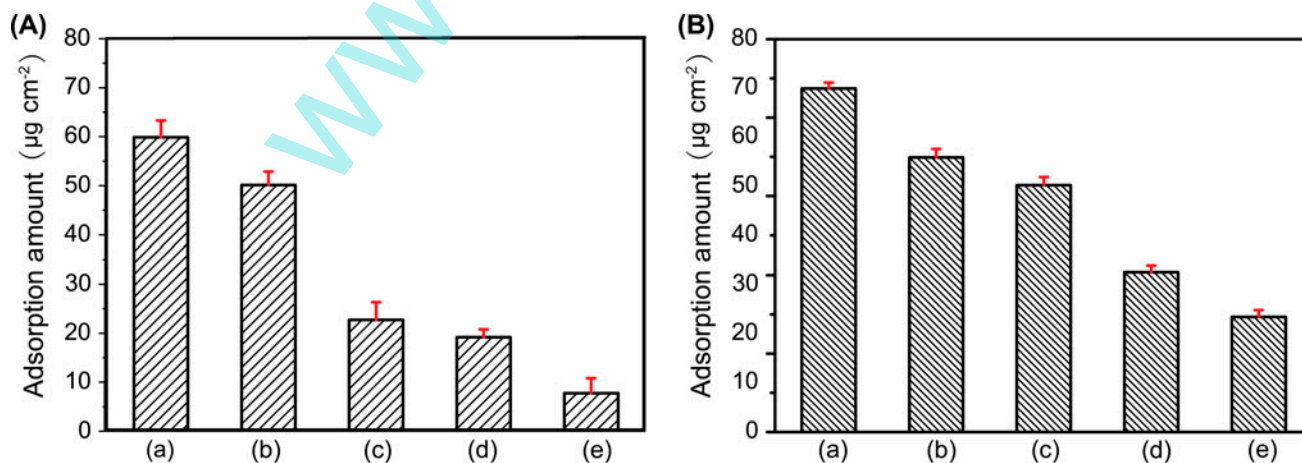

Figure 12.   Static adsorption amounts of (A) proteins and (B) polysaccharides on the PVDF-g-PDMAEMA membrane treated with 1,3-PS for (a) 0 h, (b) 8 h, (c) 24 h, (d) 48 h and (e) 96 h.
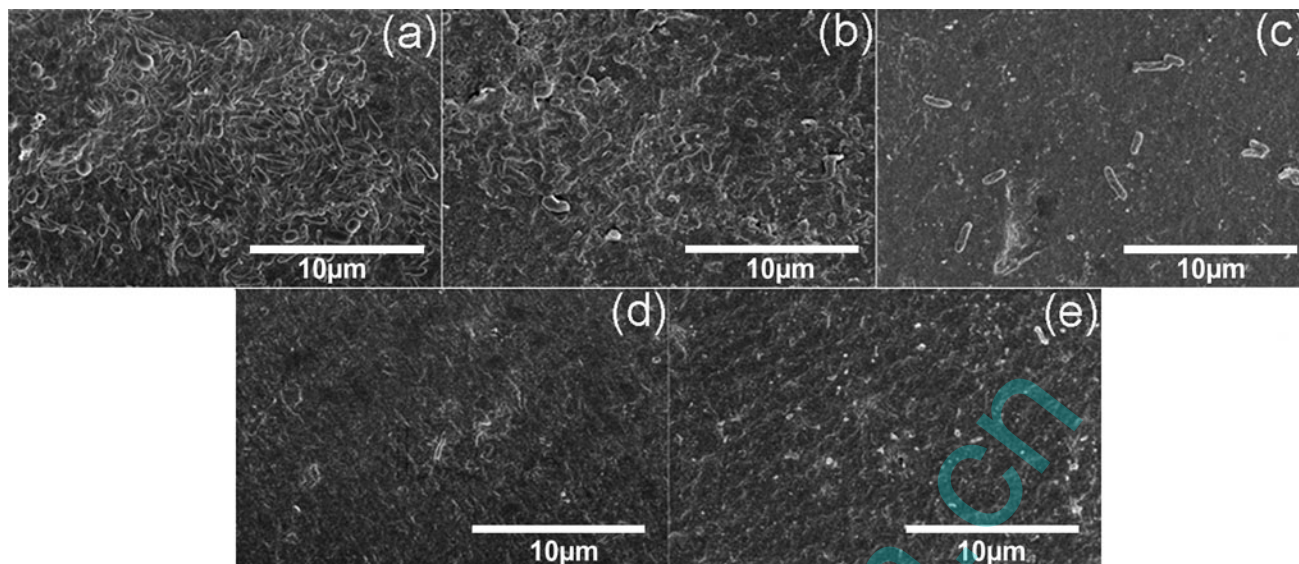
Figure 13. Typical FESEM images after adhesion of *E. coli* to the PVDF-g-PDMAEMA membrane treated with 1,3-PS for (a) 0 h, (b) 8 h, (c) 24 h, (d) 48 h and (e) 96 h.

on the surface of the pristine PVDF-g-PDMAEMA membrane. After zwitterionization, the adhesion of bacteria to the membrane surface was suppressed. For the membrane treated for 48 and 96 h, no bacteria were observed, demonstrating an excellent resistance to biofouling. These results confirmed that the incorporation of zwitterions into the surface of the membrane made bacterial attachment difficult.

Filtration of the bacterial suspension

To further investigate bacterial adhesion, all the membranes are utilized to filter a suspension of *E. coli*. The filtration process can be divided into three stages. The first stage ($J_{w, 0}$) was the filtration of pure water; the second stage (J_p) was the filtration of the bacterial suspension; and the third stage ($J_{w, 1}$), after the membrane had been washed with water, was the steady passing of pure water. The initial flux of pure water decreased from 290.0 ± 4 to $240.5 \pm 5.1\,l\,m^{-2}\,h^{-1}$ when the treatment time increased from 0 to 96 h (Figure 14). A lower pure water flux resulted from the smaller pore size and porosity of membranes, as shown in Figure 8.

FR$_w$ was introduced to evaluate the recovery property of the prepared membranes. The FR$_w$ of membranes treated with 1,3-PS was higher than that of the pristine PVDF-g-PDMAEMA membrane (Figure 15). For the 96 h treatment, the FR$_w$ reached 93.4%, indicating a high recycling property. The number of bacterial cells on the surface of the membrane was reduced because hydration layers prevented the deposition of bacterial cells during the filtration process. In addition, the bacterial cells were displaced from the pore surface after flushing with water. This reduced the severity of pore blockages and thus a
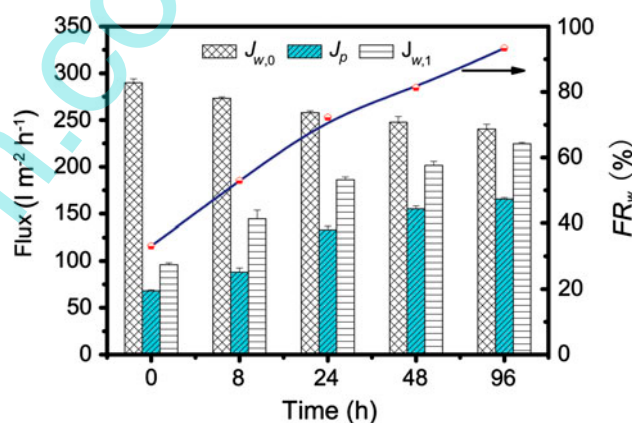

Figure 14. Filtration performance of the membranes. $J_{w, 0}$ is the steady flux of pure water. J_p is the flux of the bacterial suspension and $J_{w,1}$ is the flux of pure water after the bacterial suspension was filtered through the membranes. FR$_W$ is the flux recovery during the filtration cycle.

relatively higher FR$_w$ was obtained. To further analyse the membrane fouling during the filtration process, the value of R_t, R_r and R_{ir} was calculated using Equations 3–5. The total membrane fouling (R_t) was the sum of the reversible fouling ratio (R_r) and the irreversible fouling ratio (R_{ir}). By hydraulic cleaning, the R_r could be recovered but the R_{ir} could not. The R_t decreased from 78 to 32% with the increase in treatment time from 0 to 96 h, which indicates that the zwitterionic membranes could maintain a lower fouling (Figure 15). To further analyse the membrane fouling, the ratio of reversible fouling to irreversible fouling in the filtration process (R_r/R_{ir}) was calculated. The R_r/R_{ir} value increased from 0.14 to 3.71
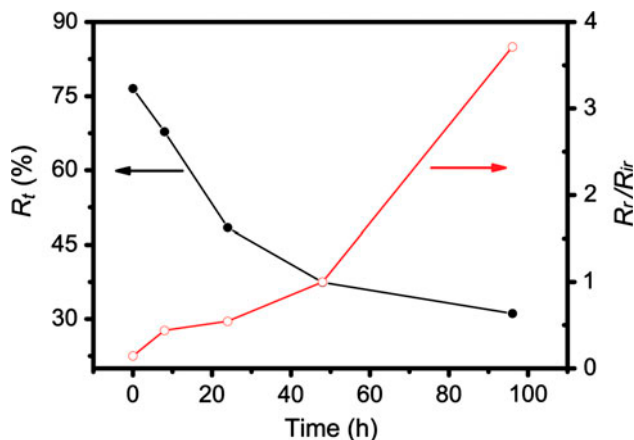
Figure 15. R_t and R_r/R_{ir} of PVDF-g-PDMAEMA membranes treated with 1,3-PS for different periods.

with the increase in treatment time from 0 to 96 h, indicating that fouling was more reversible after the zwitterions were incorporated into the membrane surface. As a result, the zwitterionic membranes could recover a high water flux after hydraulic cleaning and exhibited excellent biofouling resistance in the filtration process.

Conclusions

A copolymer of PVDF grafted with PDMAEMA side chains was successfully synthesized, and a flat membrane was prepared *via* immersed phase inversion. An approach to yield an anti-biofouling surface was provided through transformation of aggregated PDMAEMA chains into zwitterions with 1,3-PS as the quaternization agent. The zwitterions were distributed not only on the membrane surface but also on the surface of the internal channels. This was confirmed by the decreasing roughness parameters, the mean pore size and the porosity of the membranes. The incorporation of zwitterions into the membrane surface resulted in limited EPS adsorption and bacterial adhesion. Therefore, zwitterionic PVDF membranes exhibited good resistance to biofouling.

Acknowledgements

References

Bazaka K, Jacob MV, Crawford RJ, Ivanova EP. 2012. Efficient surface modification of biomaterial to prevent biofilm formation and the attachment of microorganisms. Appl Microbiol Biotechnol. 95:299–311.

Berndt E, Behnke S, Dannehl A, Gajda A, Wingender J, Ulbricht M. 2010. Functional coatings for anti-biofouling applications by surface segregation of block copolymer additives. Polymer. 5:5910–5920.

Chang Y, Chang WJ, Shih YJ, Wei TC, Hsiue GH. 2011. Zwitterionic sulfobetaine-grafted poly(vinylidene fluoride) membrane with highly effective blood compatibility *via* atmospheric plasma-induced surface copolymerization. ACS Appl Mater Interfaces. 3:1228–1237.

Chen SF, Jiang SY. 2008. A new avenue to non fouling materials. Adv Mater. 20:335–338.

Cheng G, Li GZ, Xue H, Chen SF, Bryers JD, Jiang SY. 2009. Zwitterionic carboxybetaine polymer surfaces and their resistance to long-term biofilm formation. Biomaterials. 30:5234–5240.

Chiang YC, Chang Y, Higuchi A, Chen WY, Ruaan RC. 2009. Sulfobetaine-grafted poly(vinylidene fluoride) ultrafiltration membranes exhibit excellent antifouling property. J Membr Sci. 339:151–159.

Deng B, Yu M, Yang XX, Zhang BW, Li LF, Xie LD, Li JY, Lu XF. 2010. Antifouling microfiltration membranes prepared from acrylic acid or methacrylic acid grafted poly (vinylidene fluoride) powder synthesized *via* pre-irradiation induced graft polymerization. J Membr Sci. 350:252–258.

Dong CX, He GH, Li H, Zhao R, Han Y, Deng YL. 2012. Antifouling enhancement of poly(vinylidene fluoride) microfiltration membrane by adding $Mg(OH)_2$ nanoparticles. J Membr Sci. 387–388:40–47.

Dubois M, Gilles KA, Hamilton JK, Rebers PA, Smith F. 1956. Colorimetric method for determination of sugars and related substances. Anal Chem. 28:350–356.

Eboigbodin KE, Biggs CA. 2008. Characterization of the extracellular polymeric substances produced by *Escherichia coli* using infrared spectroscopic, proteomic, and aggregation studies. Biomacromolecules. 9:686–695.

Feng X, Guo YF, Chen X, Zhao YP, Li JX, He XL, Chen L. 2012. Membrane formation process and mechanism of PVDF-g-PNIPAAm thermo-sensitive membrane. Desalination. 290:89–98.

Guo YF, Feng X, Chen L, Zhao YP, Bai JN. 2010. Influence of the coagulation-bath temperature on the phase-separation process of poly(vinylidene fluoride)-graft-poly(*N*-isopropyl-acrylamide) solutions and membrane structures. J Appl Polym Sci. 116:1005–1009.

Hamzah S, Ali N, Mohammad A, Ariffin M., Ali A. 2012. Design of chitosan/PSf self-assembly membrane to mitigate fouling and enhance performance in trypsin separation. J Chem Technol Biotechnol. 87:1157–1166.

Herzberg M, Berry D, Raskin L. 2010. Impact of microfiltration treatment of secondary wastewater effluent on biofouling of reverse osmosis membranes. Water Res. 44:167–176.

Herzberg M, Sweity A, Brami M, Kaufman Y, Freger V, Oron G, Belfer S, Kasher R. 2011. Surface properties and reduced biofouling of graft-copolymers that possess oppositely charged groups. Biomacromolecules. 12:1169–1177.

Kaneko H, Funatsu K. 2012. Visualization of models predicting transmembrane pressure jump for membrane bioreactor. Ind Eng Chem Res. 51:9679–9686.

Khayet M, García-Payo MC, Qusay FA, Zubaidy MA. 2009. Structural and performance studies of poly(vinyl chloride) hollow fiber membranes prepared at different air gap lengths. J Membr Sci. 330:30–39.

Khulbe KC, Feng CY, Hamad F, Matsuura T, Khayet M. 2004. Structural and performance study of micro porous polyetherimide hollow fiber membranes prepared at different air-gap. J Membr Sci. 245:191–198.

Kim YW, Lee DK, Lee KJ, Kim JH. 2008. Single-step synthesis of proton conducting poly(vinylidene fluoride) (PVDF) graft copolymer electrolytes. Eur Polym J. 44:932–939.

Koh JK, Kim YW, Ahn SH, Min BR, Kim JH. 2010. Antifouling poly(vinylidene fluoride) ultrafiltration membranes containing amphiphilic comb polymer additive. J Polym Sci, Part B: Polym Phys. 48:183–189.

Kovalova L, Siegrist H, Singer H, Wittmer A, McArdell CS. 2012. Hospital wastewater treatment by membrane bioreactor: performance and efficiency for organic micro pollutant elimination. Environ Sci Technol. 46:1536–1545.

Li JH, Li MZ, Miao J, Wang JB, Shao XS, Zhang QQ. 2012. Improved surface property of PVDF membrane with amphiphilic zwitterionic copolymer as membrane additive. Appl Surf Sci. 258:6398–6405.

Li MZ, Li JH, Shao XS, Miao J, Wang JB, Zhang QQ, Xu XP. 2012. Grafting zwitterionic brush on the surface of PVDF membrane using physisorbed free radical grafting technique. J Membr Sci. 405–406:141–148.

Li Q, Bi QY, Zhou B, Wang XL. 2012. Zwitterionic sulfobetaine-grafted poly(vinylidene fluoride) membrane surface with stably anti-protein-fouling performance *via* a two-step surface polymerization. Appl Surf Sci. 258:4707–4717.

Lowe AB, Billingham NC, Armes SP. 1996. Synthesis of polybetaines with narrow molecular mass distribution and controlled architecture. Chem Commun. 13:1555–1556.

Lowe AB, McCormick CL. 2002. Synthesis and solution properties of zwitterionic polymers. Chem Rev. 102:4177–4189.

Ma CF, Zhou H, Wu B, Zhang GZ. 2011. Preparation of polyurethane with zwitterionic side chains and their protein resistance. ACS Appl Mater Interfaces. 3:455–461.

McGinty KM, Brittain WJ. 2008. Hydrophilic surface modification of poly(vinyl chloride) film and tubing using physisorbed free radical grafting technique. Polymer. 49:4350–4357.

Qin L, Zhang GL, Meng Q, Xu LS, Lv BS. 2012. Enhanced MBR by internal micro-electrolysis for degradation of anthraquinone dye wastewater. Chem Eng J. 210:575–584.

Rahimpour A, Madaeni SS. 2010. Improvement of performance and surface properties of nano-porous polyethersulfone (PES) membrane using hydrophilic monomers as additives in the casting solution. J Membr Sci. 360:371–379.

Razi F, Sawada I, Ohmukai Y, Maruyama T, Matsuyama H. 2012. The improvement of antibiofouling efficiency of polyethersulfone membrane by functionalization with zwitterionic monomers. J Membr Sci. 401–402:292–299.

Samanta S, Chatterjee DP, Manna S, Mandal A, Garai A, Nandi AK. 2009. Multifunctional hydrophilic poly(vinylidene fluoride) graft copolymer with supertoughness and supergluing properties. Macromolecules. 42:3112–3120.

Schepelina O, Zharov I. 2008. Poly(2-(dimethylamino)ethyl methacrylate)-modified nanoporous colloidal films with pH and ion response. Langmuir. 24:14188–14194.

Sheng GP, Yu HQ, Yu Z. 2005. Extraction of extracellular polymeric substances from the photosynthetic bacterium *Rhodopseudomonas acidophila*. Appl Microbiol Biotechnol. 67:125–130.

Sim STV, Suwarno SR, Chong TH, Krantz WB, Fane AG. 2013. Monitoring membrane biofouling *via* ultrasonic time-domain reflectometry enhanced by silica dosing. J Membr Sci. 428:24–37.

Sui Y, Wang ZN, Gao XL, Gao CJ. 2012. Antifouling PVDF ultrafiltration membranes incorporating PVDF-g-PHEMA additive *via* atom transfer radical graft polymerizations. J Membr Sci. 413–414:38–47.

Takagi R, Hori M, Gotoh K, Tagawa M, Nakagaki M. 2000. Donnan potential and ζ-potential of cellulose acetate membrane in aqueous sodium chloride solutions. J Membr Sci. 170:19–25.

Tao MM, Liu F, Xue LX. 2012. Hydrophilic poly(vinylidene fluoride) (PVDF) membrane by *in situ* polymerisation of 2-hydroxyethyl methacrylate (HEMA) and micro-phase separation. J Mater Chem. 22:9131–9137.

Vaisocherová H, Yang W, Zhang Z, Cao ZQ, Cheng G, Piliarik M, Homola J, Jiang SY. 2008. Ultralow fouling and functionalizable surface chemistry based on a zwitterionic polymer enabling sensitive and specific protein detection in undiluted blood plasma. Anal Chem. 80:7894–7901.

Venault A, Chang Y, Wang DM, Bouyer D, Higuchi A, Lai JY. 2012. PEGylation of anti-biofouling polysulfone membranes *via* liquid- and vapor-induced phase separation processing. J Membr Sci. 403–404:47–57.

Wang PP, Ma J, Wang ZH, Shi FM, Liu QL. 2012. Enhanced separation performance of PVDF/PVP-g-MMT nanocomposite ultrafiltration membrane sased on the NVP-grafted polymerization modification of montmorillonite (MMT). Langmuir. 28:4776–4786.

Yang XX, Zhang BW, Liu ZY, Deng B, Yu M, Li LF, Jiang HQ, Li JY. 2011. Preparation of the antifouling microfiltration membranes from poly(*N,N*-dimethylacrylamide) grafted poly(vinylidene fluoride) (PVDF) powder. J Mater Chem. 21:11908–11915.

Yi Z, Zhu LP, Xu YY, Gong XN, Zhu BK. 2011. Surface zwitterionicalization of poly(vinylidene fluoride) porous membranes by post-reaction of the amphiphilic precursor. J Membr Sci. 385–386:57–66.

Zhai GQ, Kang ET, Neoh KG. 2004. Inimer graft-copolymerized poly(vinylidene fluoride) for the preparation of arborescent copolymers and 'surface-active' copolymer membranes. Macromolecules. 37:7240–7249.

Zhu ZZ, Luo JQ, Ding LH, Bals O, Jaffrin MY, Vorobiev E. 2013. Chicory juice clarification by membrane filtration using rotating disk module. J Food Eng. 115:264–271.